A

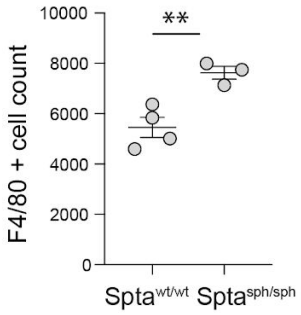


B

| marker gene | cell population |
|---|---|
| Cd68 | Kupffer cells |
| Adgre1 | Kupffer cells |
| Clec4f | Kupffer cells |
| Sparc | endothelial cells |
| Kdr | endothelial cells |
| F8 | endothelial cells |
| Clec4g | endothelial cells |
| Dcn | hepatocytes |
| Apoa2 | hepatocytes |
| Ttr | hepatocytes |
| Epor | erythroblastic island macrophages |
| Klf1 | erythroblastic island macrophages |
| S100a11 | early recruited macrophages |
| Ccr2 | early recruited macrophages |
| Itgam | early recruited macrophages |
| S100a6 | early recruited macrophages |

C

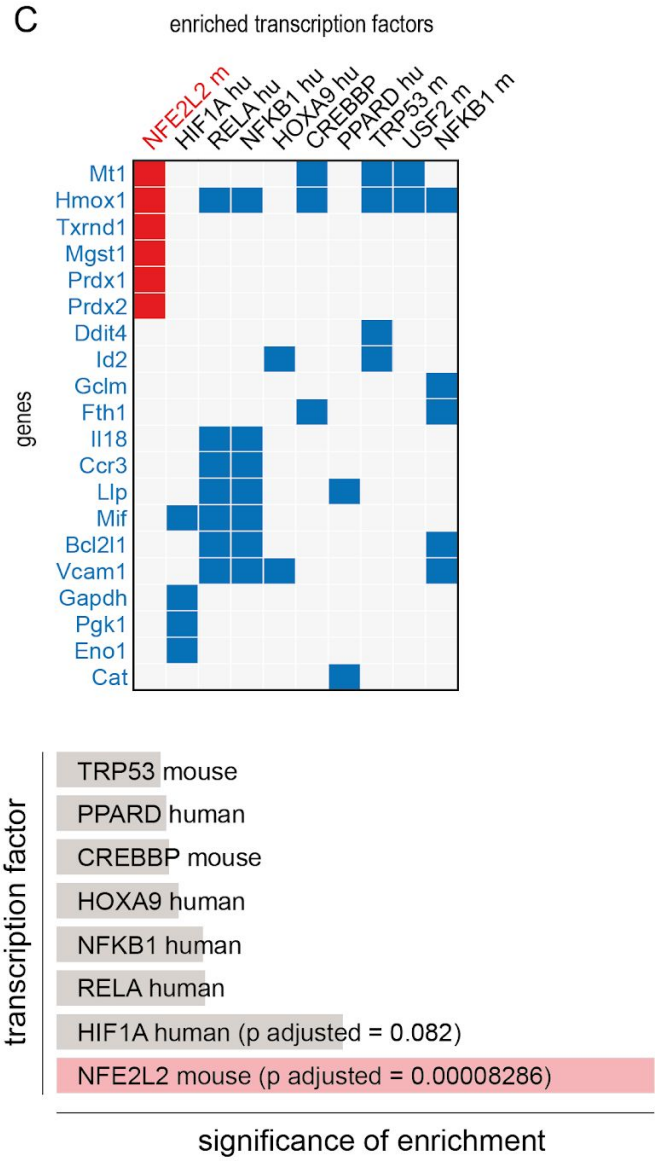


**Supplementary Figure 1**

A. Number of F4/80 positive liver macrophages in *Spta*$^{sph/sph}$ and *Spta*$^{wt/wt}$ mice quantified on histology images of liver microtome sections stained with an anti-F4/80 antibody (n=3-4).
B. Gene markers for each cell population identified in the single-cell RNA sequencing (scRNA-seq) of F4/80-enriched nonparenchymal liver cell suspensions isolated from one *Spta*$^{sph/sph}$ and one *Spta*$^{wt/wt}$ mouse.
C. EnrichR analysis of the significantly differentially expressed genes (DEGs) (log2FC > 0.5, *p*-value < 0.01) between the *Spta*$^{sph/sph}$ and *Spta*$^{wt/wt}$ KCs obtained by scRNA-seq. Heatmap showing the associations between the input genes and the overlapping genes of the top 10 enriched terms. The enriched terms in the columns of the matrix are ranked based on their *p*-value.

Individual symbols represent one mouse; ** p<0.01 for all panels, using a two sample t-test.

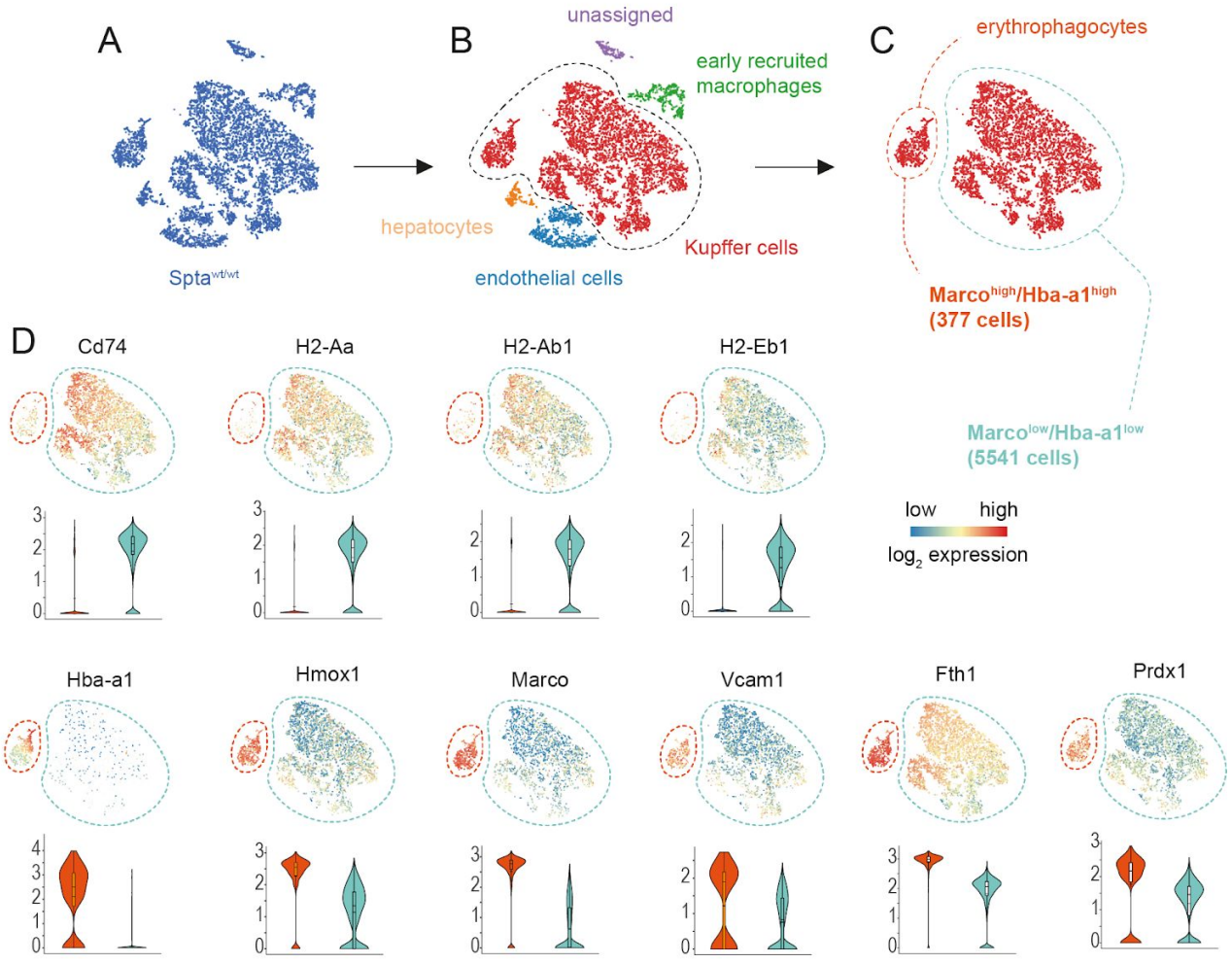


**Supplementary Figure 2**

ScRNA-seq was performed on F4/80-enriched nonparenchymal liver cell suspensions isolated from one *Spta*$^{sph/sph}$ and one *Spta*$^{wt/wt}$ mouse. Dataset of the *Spta*$^{wt/wt}$ mouse is shown.

A. t-SNE plot showing cells colored based on cell origin (blue, *Spta*$^{wt/wt}$).
B. t-SNE plot showing cells colored based on identity.
C. t-SNE plot showing *Marco*$^{+}$ and *Marco*$^{negative}$ KCs.
D. t-SNE plots visualizing cells colored by expression of *Marco, Vcam1, Hba-a1, Hmox1, Fth1, Ftl1, Prdx1, Cd74, H2-Aa, H2-Ab1,* and *H2-Eb1* in KCs from the *Spta*$^{wt/wt}$ mouse. *Marco*$^{+}$ and *Marco*$^{negative}$ KCs are highlighted by the magenta and blue dashed lines, respectively. Legend for relative log2 expression of each gene from lowest expression (blue dots) to highest expression (red dots) is displayed on the top right.

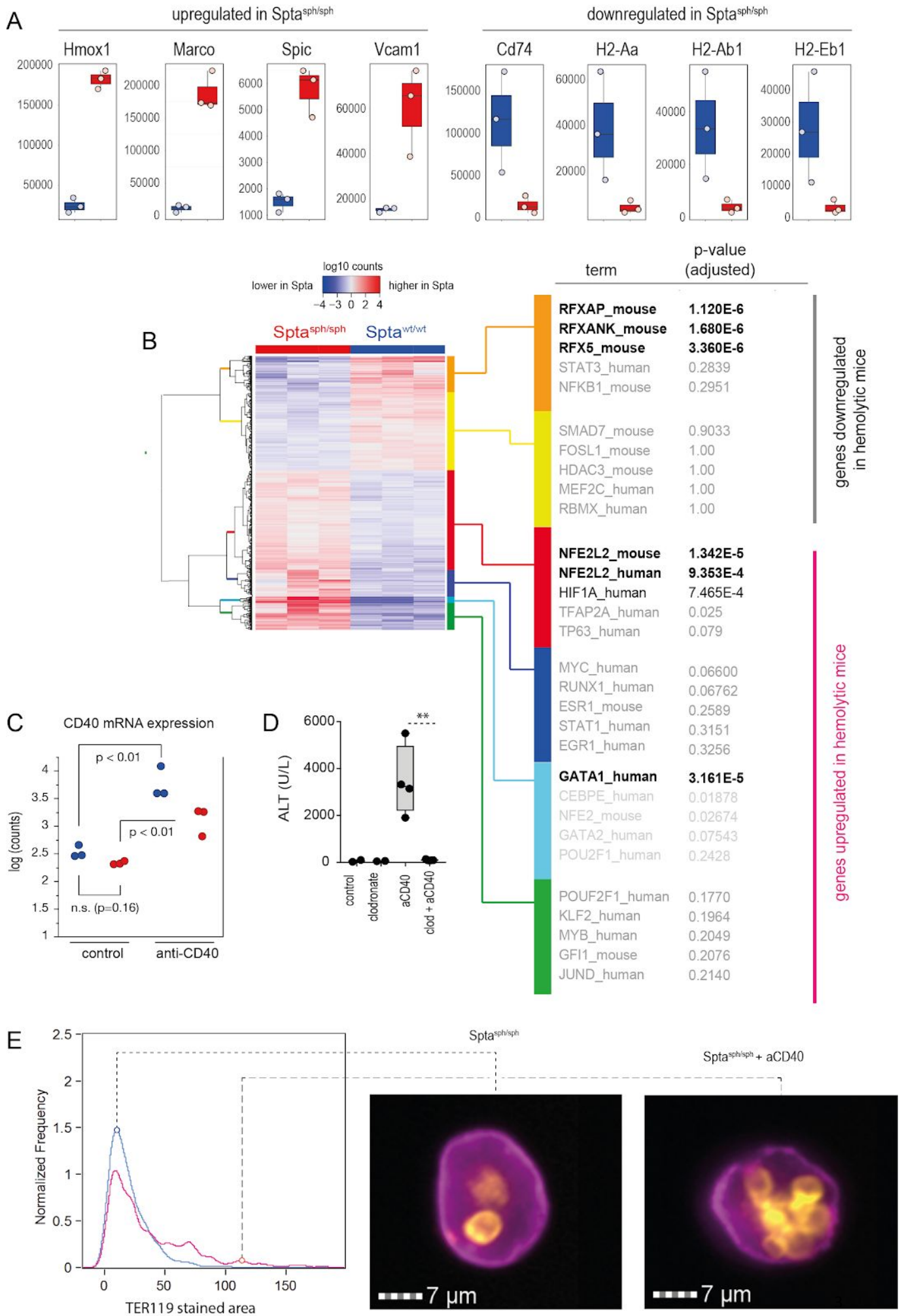
A
upregulated in Spta sph/sph
downregulated in Spta sph/sph
Hmox1
Marco
Spic
Vcam1
Cd74
H2-Aa
H2-Ab1
H2-Eb1
B
log10 counts
lower in Spta
higher in Spta
−4 −3 0 2 4
Spta sph/sph
Spta wt/wt
term
p-value (adjusted)
RFXAP_mouse 1.120E-6
RFXANK_mouse 1.680E-6
RFX5_mouse 3.360E-6
STAT3_human 0.2839
NFKB1_mouse 0.2951
SMAD7_mouse 0.9033
FOSL1_mouse 1.00
HDAC3_mouse 1.00
MEF2C_human 1.00
RBMX_human 1.00
NFE2L2_mouse 1.342E-5
NFE2L2_human 9.353E-4
HIF1A_human 7.465E-4
TFAP2A_human 0.025
TP63_human 0.079
MYC_human 0.06600
RUNX1_human 0.06762
ESR1_mouse 0.2589
STAT1_human 0.3151
EGR1_human 0.3256
GATA1_human 3.161E-5
CEBPE_human 0.01878
NFE2_mouse 0.02674
GATA2_human 0.07543
POU2F1_human 0.2428
POUF2F1_human 0.1770
KLF2_human 0.1964
MYB_human 0.2049
GFI1_mouse 0.2076
JUND_human 0.2140
genes downregulated in hemolytic mice
genes upregulated in hemolytic mice
C
CD40 mRNA expression
p < 0.01
p < 0.01
n.s. (p=0.16)
log (counts)
control
anti-CD40
D
ALT (U/L)
**
control
clodronate
aCD40
clod + aCD40
E
Normalized Frequency
TER119 stained area
Spta sph/sph
Spta sph/sph + aCD40
7 µm
7 µm

**Supplementary Figure 3**

A. Bulk RNA-sequencing (bulk RNA-seq) data of F4/80-enriched nonparenchymal liver cell suspensions isolated from *Spta*$^{sph/sph}$ and *Spta*$^{wt/wt}$ mice (n=3). Normalized count data of signature genes in *Spta*$^{sph/sph}$ (red) and *Spta*$^{wt/wt}$ (blue) are plotted.

B. Hierarchical clustering analysis of the 1564 significant DEGs ( log2FC > 0.5, *p*-value < 0.01, rows) between the *Spta*$^{sph/sph}$ and *Spta*$^{wt/wt}$ KCs (column) obtained by bulk RNA-seq. The significant DEGs of each subcluster were input into EnrichR, and the top five transcription factor terms identified in each subcluster are shown (blue=low expression, red=high expression).

C. Normalized log count data of *Cd40* expression in liver macrophages of *Spta*$^{sph/sph}$ and *Spta*$^{wt/wt}$ mice (n=3).

D. Plasma concentrations of alanine aminotransferase (ALT) in saline- or anti-CD40-treated C57BL/6J mice subjected or not subjected to macrophage depletion with liposomal clodronate (n=2-4).

E. **Left panel**: Histogram of the area per cell occupied by TER119$^{pos}$ erythrocytes (object) internalized by F4/80$^{pos}$ KCs from saline-or anti-CD40-treated *Spta*$^{sph/sph}$. **Right panel**: Corresponding fluorescent images showing intracellular TER119$^{pos}$ erythrocytes (yellow) in F4/80$^{pos}$ KCs (purple) from saline or anti-CD40-treated *Spta*$^{sph/sph}$ mice obtained by imaging flow cytometry.

Individual symbols represent one mouse; *** p<0.001, ** p<0.01, * p<0.05 for all panels using EdgeR for panel C, ANOVA with Tukey's post hoc test for panel D.

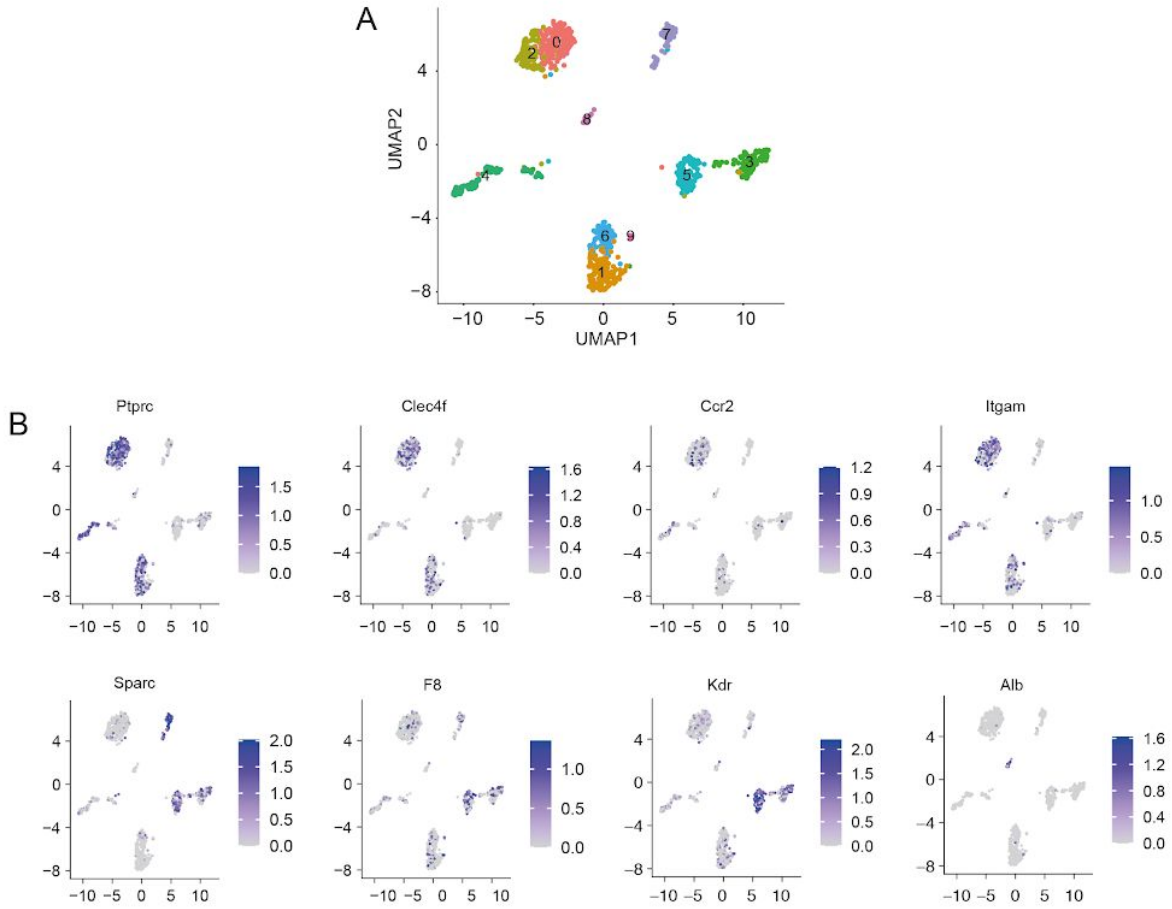


**Supplementary Figure 4**

Single Cell ATAC sequencing data of nonparenchymal liver cell suspensions enriched for macrophages with F4/80 antibody-coated magnetic Dynabeads from *Spta*$^{sph/sph}$ and *Spta*$^{wt/wt}$ mice.

A. UMAP plots showing all cells colored by cluster. In total, 9 clusters were identified, numbered from largest cluster to smallest, based on the different peak fragments displayed.
B. UMAP plots showing all cells colored by specific cell type gene markers: *Ptprc*, *Clec4f* for KCs; *Ccr2*, *Itgam* for early recruited macrophages; *Sparc*, *F8*, *Kdr* for endothelial cells; *Alb* for hepatocytes.

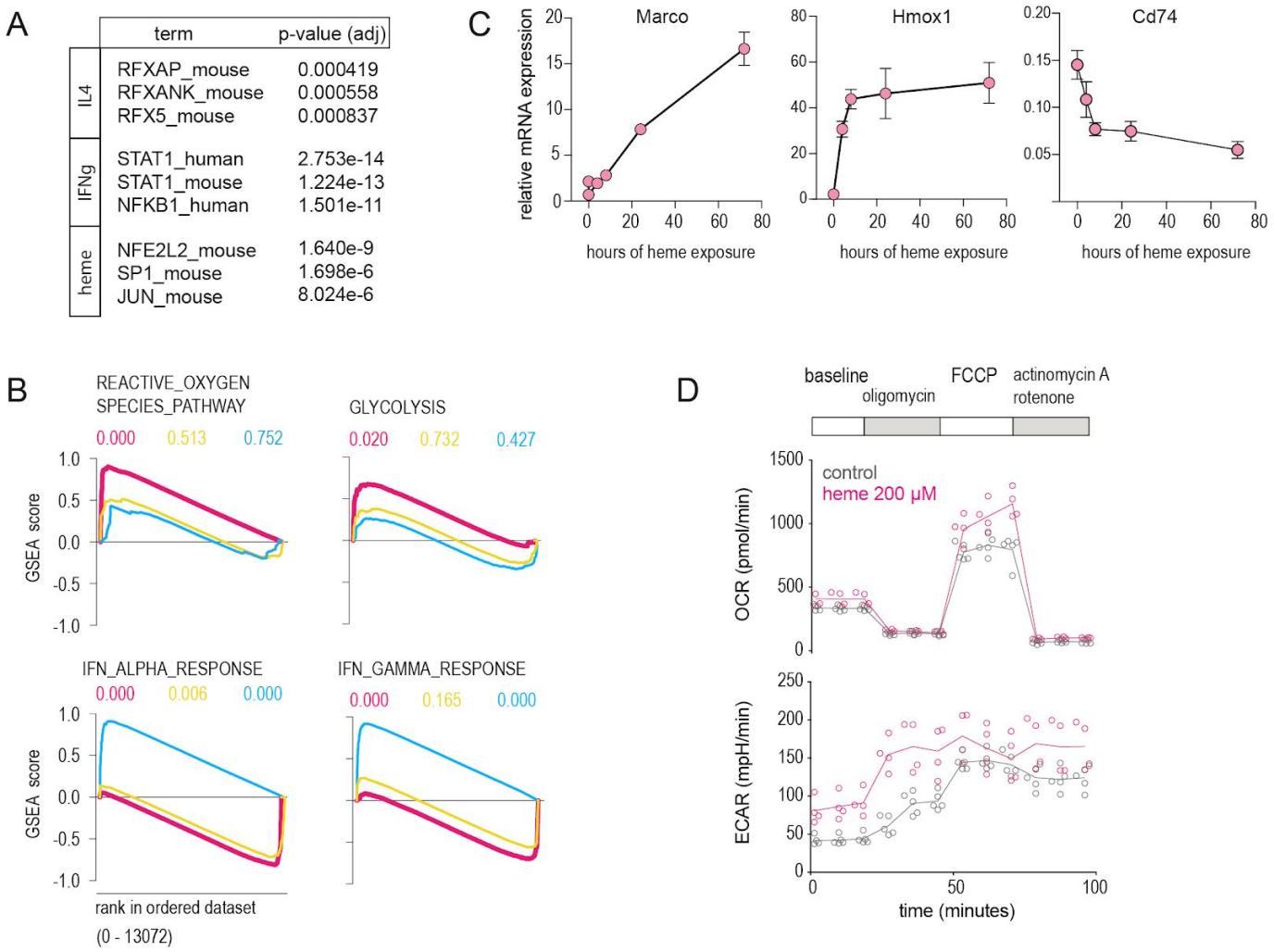


**Supplementary Figure 5**

A. Results of EnrichR analysis for transcription factors of all the significantly upregulated genes in mouse BMDMs stimulated with IL-4, IFN $\gamma$ or heme-albumin (200 µM). The top three significant transcription factors are displayed for each condition. With the thresholds of log2FC > 0.5 and *p*-value < 0.01, 2593 significant DEGs were detected in heme-albumin-treated BMDMs, 3290 in IFN $\gamma$ -treated BMDMs and 2886 in IL-4-treated BMDMs compared to the respective control.

B. Overlaid GSEA enrichment score plots of the differential gene expression effects of IFN $\gamma$ (blue)-, IL-4- (yellow) and heme-albumin (magenta)-treated BMDMs. The positively (left) and negatively (right) enriched gene sets are shown. Plots display running enrichment score and position of gene set members on the rank ordered list. At the top of each plot, the adjusted *p*-values are displayed, color-coded for each condition .

C. mRNA expression of *Hmox1, Marco,* and *Cd74* measured by RT-qPCR in mouse BMDMs treated with albumin (control) or heme-albumin (200 µM) for 4, 8, 24 and 72 hours (every dot represents the mean of 4 experiments +/- SEM).

D. Oxygen consumption rate (OCR) and extracellular acidification rate (ECAR) of heme-albumin (200 µM)-exposed and albumin(control) BMDMs were measured using a Seahorse XFe24 extracellular flux analyzer. Measurements (n=3) were recorded according to the standard protocol at baseline, after addition of *oligomycin* (an inhibitor of ATP synthase), after addition of *carbonyl cyanide-4 (trifluoromethoxy) phenylhydrazone (FCCP)* (an uncoupling agent, which allows to measure maximum mitochondrial oxygen consumption), and after addition of combined *actinomycin A and rotenone* (which shuts down mitochondrial respiration).

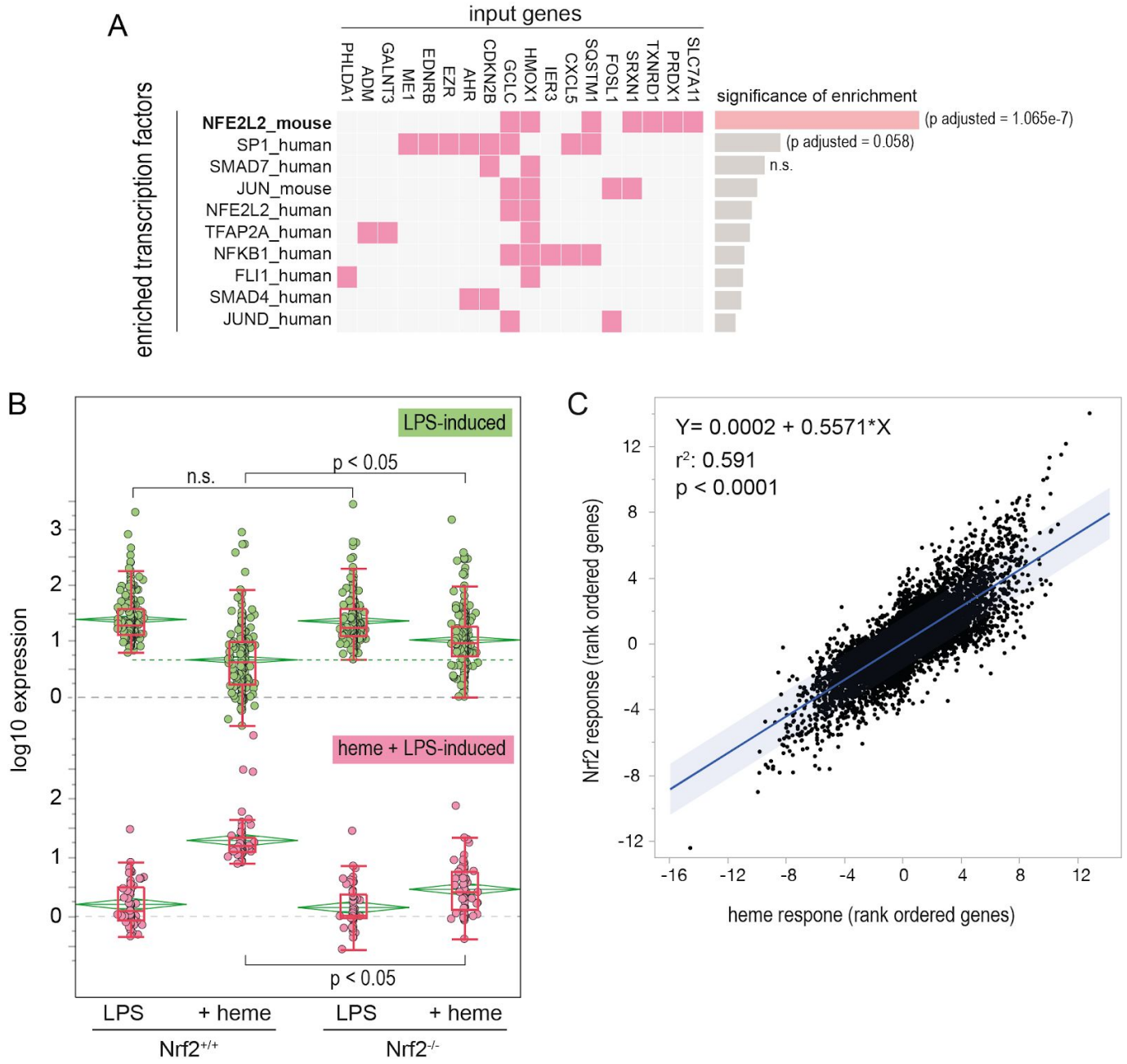


**Supplementary Figure 6**

A. EnrichR analysis for transcription factors of the positive DEGs (log2FC > 0.5, *p*-value < 0.01) by heme-albumin stimulation in wild-type BMDMs (effect$_{heme}$) identified in Figure 6B. Heatmap showing the associations between the input genes and the overlapping genes of the top 10 enriched transcription factors. The enriched terms in the columns of the matrix are ranked based on their *p*-value.

B. Expression data illustrating the levels of LPS-induced genes (green) and heme + LPS-induced genes (magenta) in wild-type and *Nrf2*$^{-/-}$ BMDMs after stimulation with LPS alone or LPS + heme-albumin (same gene as shown in Figure 6B). In the absence of extracellular heme, *Nrf2* knockout and wild-type macrophages exhibit comparable responses after LPS treatment. However, the heme-albumin-mediated suppression of LPS-induced genes was significantly attenuated in *Nrf2*$^{-/-}$ macrophages compared to wild-type macrophages.

C. Scatterplot displaying the rank (*-log (pvalue)*) of each gene in the *Nrf2*-response versus the heme-response dataset (every point represents a gene). These data represent the input data for the GSEA analysis that is shown in Figure 6D.

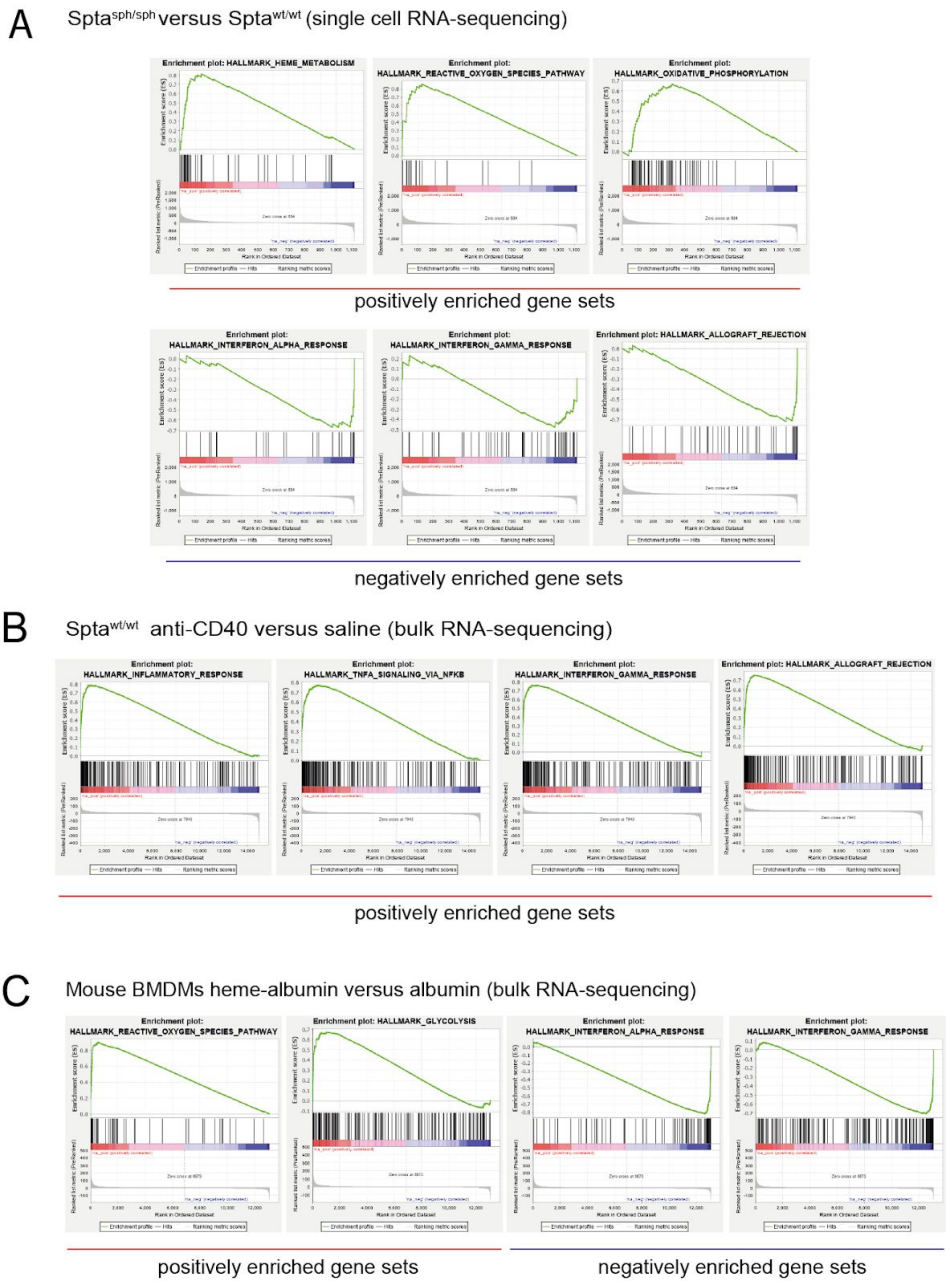


**Supplementary Figure 7**

A. DEGs between liver macrophages from *Spta*$^{sph/sph}$ and *Spta*$^{wt/wt}$ mice (scRNA-seq data, Figures 1 and 2) were computed by gene set enrichment analysis (GSEA). Enrichment plots of the top three positively (top) and negatively (bottom) enriched hallmark gene sets are shown. Plots display running enrichment scores and positions of gene set members on the rank ordered list.

B. DEGs between liver macrophages from *Spta*$^{wt/wt}$ mice treated with anti-CD40 and *Spta*$^{wt/wt}$ mice treated with saline (bulk RNA-seq data, Figure 4) were computed by GSEA. Enrichment plots of the top four positively enriched hallmark gene sets are shown. Plots display running enrichment scores and positions of gene set members on the rank ordered list.

C. DEGs between BMDMs treated with heme-albumin and BMDMs treated with albumin alone (bulk RNA-seq data, Figure 5) were computed by GSEA. Enrichment plots of the top two positively (left) and negatively (right) enriched hallmark gene sets are shown. Plots display running enrichment scores and positions of gene set members on the rank ordered list.

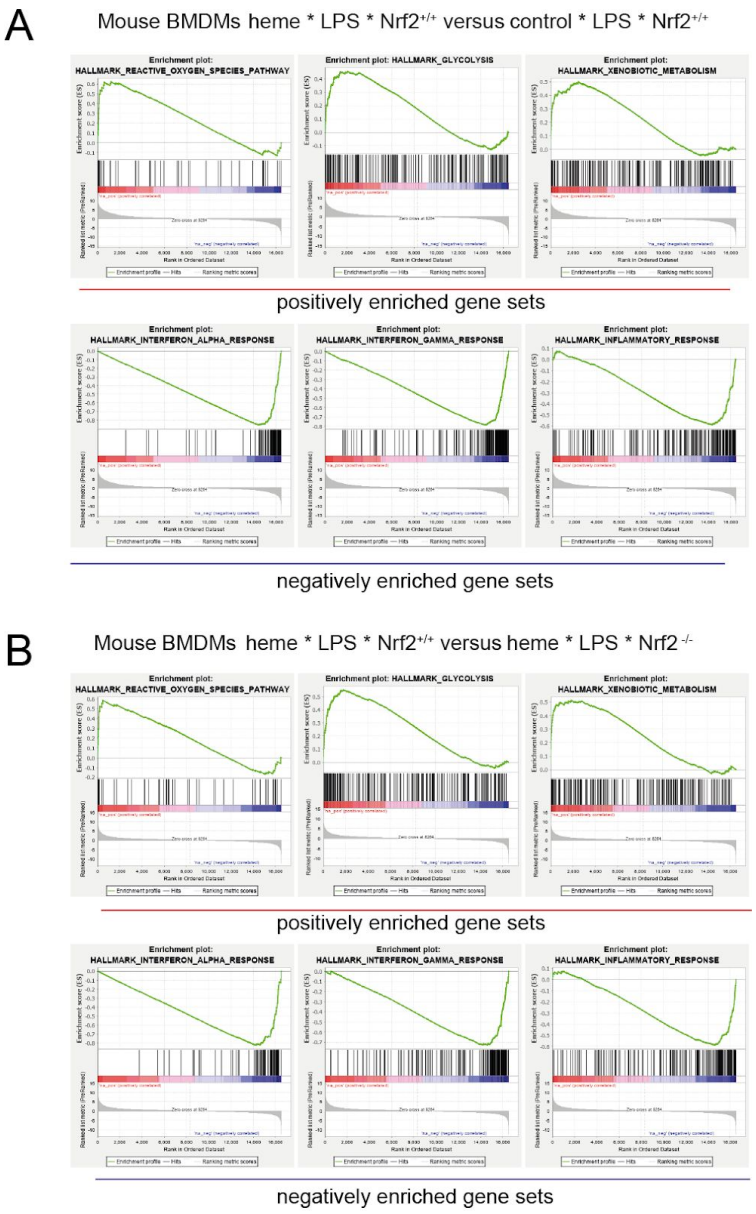


**Supplementary Figure 8**

A. DEGs between Nrf2$^{+/+}$ BMDMs treated with heme-albumin + LPS and Nrf2$^{+/+}$ BMDMs treated with albumin + LPS (microarray, Figure 6) were computed by GSEA. Enrichment plots of the top three positively (top) and negatively (bottom) enriched hallmark gene sets are shown. Plots display running enrichment score and position of gene set members on the rank ordered list.

B. DEGs between Nrf2$^{+/+}$ and Nrf2$^{-/-}$ BMDMs treated with heme-albumin + LPS (microarray data, Figure 6) were computed by GSEA. Enrichment plots of the top three positively (top) and negatively (bottom) enriched hallmark gene sets are shown. Plots display running enrichment scores and positions of gene set members on the rank ordered list.

## SUPPLEMENTARY METHODS

### *Mouse models/interventions*

***Anti-CD40 antibody-induced systemic inflammation and hepatitis model:*** Mice were treated intraperitoneally (i.p.) with 20 mg/kg agonistic anti-CD40 antibody (InVivoPlus, clone FGK4.5/FGK45). Thirty hours after anti-CD40 injection, blood was removed by terminal heart puncture for ALT (Reflotron ALT 10745138, Roche) or cytokine measurement (Bio-rad, Bioplex); livers were collected 48 hours after anti-CD40 injection.

***Liposomal clodronate injections (macrophage depletion):*** To selectively isolate liver KCs, mice were given two i.p. doses of 150-200 µl of clodronate liposomes (Clophosome®-A-Clodronate Liposomes (Anionic), FormuMax, F70101C-A) on days 1 and 4. Mice were injected with anti-CD40 five days after the beginning of clodronate liposome treatment and sacrificed 30 hours later.

***MCD diet model:*** Mice were fed an MCD diet (TD.90262, Harlan Laboratories) or a control diet (TD.94149) for 12 days. The body weight of the animals was measured at days 0, 3, 6, 10, 11 and 12. At day 12, mice were sacrificed for terminal heart puncture (ALT and CCL2 measurement), macrophage isolation or liver collection.

***Dimethyl fumarate (DMF) treatment:*** DMF (Alfa Aesar, A10402.30) was suspended in a solution of 0.8% Methyl-Cellulose (Sigma, M0512-100G) and 30% sweetened condensed milk at a concentration of 20 mg/ml and stored at 4°C for a maximum of 5 days. The drug was administered orally by micropipette guiding (1). Mice were treated twice daily with either DMF suspension (100 mg/kg) or vehicle control (0,8% Methyl-Cellulose + 30% sweetened condensed milk) from 7 days prior to MCD challenge.

***Red blood cell isolation for analysis of hemoglobin transcripts:*** Blood was sampled by terminal heart puncture from mice in heparin coated tubes (Microvette$^{R}$, Sarstedt). To deplete blood from CD45$^{+}$ leukocytes, Dynabeads Sheep anti-Rat IgG (Invitrogen, 11035), in combination with purified rat anti-mouse CD45 antibody (BD Pharmingen, 0.5 mg/ml, 103102), and a DynaMag™-2 Magnet (Thermo Fisher Scientific, 12321D) were used according to the manufacturer's negative selection protocol (Invitrogen). Whole blood was incubated with the CD45 coated Dynabeads and only the negative fraction of cells was kept for RNA extraction and RT-qPCR.

*Cell culture*

***Mouse BMDMs:*** BM cells were obtained from the femurs and tibias of 8- to 10-week-old mice. The bone marrow murine stem cells were expanded and differentiated in RPMI medium supplemented with 10% FCS in the presence of recombinant mouse M-CSF (PeproTech 315-02-100UG, lot 0914245) at 10 ng/ml for 7 days. Macrophages were polarized to the M1 phenotype with 10 ng/ml interferon gamma (IFN $\gamma$, PeproTech, 214-14-2UG, lot 111249), to the M2 phenotype with 10 ng/ml interleukin 4 (IL-4, PeproTech, 315-05-20UG, lot 061398), to erythrophagocytes-like with 200 µM or 400 µM heme-albumin or with Nuclear factor erythroid 2-related factor activators RA-839 at 15 µM (TOCRIS bioscience, 1832713-02-6, batch no 1A/185067) or ML-334 at 50 µM (TOCRIS bioscience, 1432500-66-7, batch no 1A/186673) during 72 hours of incubation. At the end of the culture period, the cells were differentiated into BMDMs, and 100% of adherent cells were positive for the F4/80 macrophage antigen measured by FACS.

***Metabolic flux analysis:*** The mitochondrial function (oxygen consumption rate) and glycolysis (acidification rate) of BMDMs were measured using a Seahorse XF24 extracellular flux analyzer and the Cell Mito Stress Kit (Agilent Technologies) according to the instructions provided by the manufacturer.

***Human monocyte-derived macrophages:*** Human-blood–derived macrophages were prepared from buffy coats of healthy donors that were purchased from a commercial provider (Swiss Red Cross; written informed consent is obtained from all donors by the Swiss Red Cross in accordance with the Declaration of Helsinki), as described previously (2). Monocytes were isolated from PBMCs by plastic adherence and cultured in Dulbecco′s Modified Eagle′s medium (DMEM, Gibco, 11880-028) supplemented with 10% pooled human serum, 1% Penicillin/Streptomycin (Gibco, 15140-122), 1% Glutamax (Gibco, 35050-061) and recombinant human M-CSF (PeproTech, 300-25, lot 021985). Heme-albumin (300 µM) was added to the medium 24 hours after plating.

*Flow cytometry and histology*

***Flow cytometry:*** Liver macrophages were preincubated with LIVE/DEAD Fixable Near-IR cell stain kit (Invitrogen, L34976) and with Mouse BD Fc Block™ (≤ 1 µg/million cells in 100 µl, BD Biosciences 553141) at 4°C and then stained with Pacific Blue anti-CD45 (5 µg/ml, BioLegend 109820), anti-F4/80 APC (5 µg/ml, BioLegend 123116) antibodies. After cell fixation with formaldehyde 2% and membrane permeabilization with permeabilization buffer

(eBioscience, 00-8333-56), ingested erythrocytes were stained intracellularly with PE anti-TER119 (2 µg/ml, Stemcell 60033) antibody. Stained cells were analyzed using an LSRFortessa (BD). Data was analyzed using FlowJo and FCS express 6 (De Novo) software. For image stream analysis, Channel 07 (Ch07, 435-505 nm), Channel 11 (Ch11, 642-745 nm) and Channel 03 (Ch03, 560-595 nm) in the ImageStream X Mk II Imaging Flow Cytometer (Amnis) were used to record Pacific Blue anti-CD45, APC anti-F4/80 and PE anti-TER119, respectively. The area occupied by ingested erythrocytes internalized by macrophages was quantified using IDEAS software.

***Immunohistochemistry:*** Liver microtome sections, 5 µm thick, were incubated overnight with a rat anti-mouse F4/80 antibody (Bio-Rad, MCA497G) diluted 1:100, followed by a biotinylated goat anti-rat secondary antibody (Vector, BA9401) diluted 1:1000. The nuclei were stained with hematoxylin. The sections were photographed with a Zeiss Apotome.2 microscope.

***Automatic quantification of hepatic steatosis:*** Macrovesicular steatosis was automatically quantified on histological images with a 10x magnification of a whole-slide scan using Fiji (3). In the first step, homogeneous bright areas with a strong border were segmented using an automatic intensity threshold combined with a simple edge detection algorithm. In the second step, the resulting particles were analyzed with regard to area and circularity ($4\pi$ (area/perimeter$^2$). Particles with an area between 25 and 1,000 µm$^2$ and a circularity >0.6 were defined as lipid droplets from macrovesicular steatosis. The summed area of all lipid droplets was then reported as a percentage of the total liver tissue.

***Automatic quantification of macrophage on liver histology section:*** The number of F4/80 positive liver macrophages was quantified on 10 randomly selected areas at 10x magnification per liver. Images were analysed using Fiji (3). Images were segmented using Yen automatic threshold selection (4, 5) on the blue channel after preprocessing with a gaussian blur (sigma = 8). The resulting particles were considered macrophages and counted with the particle analysis tool inbuilt in Fiji. For each liver, the macrophage count reported is the sum of the count in all 10 selected areas.

***Sequencing based workflows and data analysis***

***Single-cell RNA sequencing*:** Nonparenchymal liver cell suspension enriched for F4/80$^+$ macrophages were processed for library preparation according to the 10x Genomics Chromium Single Cell 3' v3 Reagent Kit instruction guide. Briefly, sample volume was

adjusted to a target capture of 10,000 cells and loaded onto the 10x Genomics single-cell-A chip. After droplet generation, samples were subjected to reverse transcriptase and the barcoded cDNA was further amplified for 11 cycles (adjusted for a cell recovery of >6000, as suggested by the 10x Genomic user guide). cDNA quality and concentration were assessed using High-Sensitivity D5000 ScreenTape (Agilent). cDNA strands were then subjected to enzymatic fragmentation, end repair and A-tailing. Adaptors were ligated to the fragmented cDNA, and sample index was added during sample index PCR (set for 12 cycles, as recommended by 10X Genomics user guide to correlate with a cDNA input of 12-150 ng). Library quality and concentration were assessed using High-Sensitivity D5000 ScreenTape (Agilent). Libraries were pooled in equimolar amounts and sequenced using the Illumina NovaSeq 6000 system according to 10X Genomics recommendations: paired-end reads, R1=28 cycles, i7=8 cycles and R2=91 cycles. Sequencing depth was targeted for 50,000 reads per cell in both samples.

***Single-cell RNA sequencing data analysis:*** The Cell Ranger Single-Cell Software Suite was used for cDNA oligopeptide alignment, barcode assignment and UMI counting from fastq data. Cell Ranger Count (version 3.0.1) generated a digital expression matrix for each sample and filtered the cell-containing droplets from empty droplets. The two filtered digital expression matrices were then merged into one using CellRanger Aggr and then further analyzed using R (v3.6.1) [https://www.R-project.org/]. Cell quality control was performed using the scater R package (v1.12.2) (6). Cells with a high mitochondrial gene ratio count were excluded from the data set (1506 out of 18,633 cells were removed). They were determined by the *isOutlier* function of the scater package, which placed the cut-off at 53% (at 3 median absolute deviation (MAD) above median of all cells). Normalization was performed using the deconvolute normalization algorithm implemented in the scran R package (v1.12.1) (7), using the *computeSumFactors* function on cells clustered with *quickCluster* function from the same package. After normalization, principal component analysis (PCA) was performed using the *denoisePCA* function of the same package to reduce the number of dimensions representing each cell. Based on the first 10 PCA, a shared nearest neighbor graph was built with the *buildSNNGraph* function, and the Louvain algorithm was performed to identify cell clusters using the *cluster_louvain* function implemented in the igraph package (v1.2.4.1). Cluster separation was assessed using modularity. Clusters were visualized using t-distributed stochastic neighbor embedding

(t-SNE) of the principal components. The top marker genes for each cluster were determined using a pairwise t-test comparing the clusters to one another using the findMarkers function of the scran package (v1.12.1). The data were visualized using BBrowser 2 with the Single-cell add on (Bioturing v2.2.4), and differential expression analysis between the liver macrophages from each mouse and those from its control was performed with the Venice function implemented in the software. Raw and processed single-cell RNA sequencing data were submitted to the Gene Expression Omnibus (GEO) database repository (8, 9).

***Bulk RNA sequencing:*** RNA was extracted from cells using the RNeasy Micro kit (Qiagen, Hombrechtikon, Switzerland) according to the manufacturer's protocol, including on-column DNase I treatment. Quality was evaluated with a spectrophotometer (NanoDrop, Thermo Fischer) and an Agilent Technologies 2100 Bioanalyzer using an RNA chip, and only samples with an RNA integrity number (RIN) of > 9 were used for sequencing. cDNA libraries were generated from the RNA samples using the Illumina TruSeq RNA stranded kit following the manufacturer's instructions. Libraries were amplified by PCR (total of 15 cycles) and their quality and concentration determined using an Agilent Fragment Analyzer with DNA High-Sensitivity Chips. The libraries were pooled in equimolar amounts and sequenced in an Illumina NovaSeq 6000 sequencer (single-end 100 bp) with a depth of approximately 20 million reads per sample.

***Bulk RNA sequencing data analysis*:** Reads were aligned to the reference genome Ensembl GRCm38.p5 Release 91 using STAR (v2.7.0e) (10). The quality of alignment was evaluated using Samtools (v1.9) (11). Counts were obtained using the *featureCounts* function of the Rsubread package (v1.22.2). Differential expression analysis was performed with the DESeq2 R package (v1.26.0) (12) or EdgeR (v 3.30.0) (13, 14) . Raw and processed bulk RNA sequencing data were submitted to the Gene Expression Omnibus (GEO) database repository (8, 9).

***Pathway and transcription factor enrichment analysis of bulk and single-cell RNA sequencing data:*** Pathway enrichment analysis was performed for the differentially expressed genes (DEGs) using the GSEA-preranked tool of the Gene set enrichment analysis (GSEA) desktop software version 4.0.2 (15). DEGs were ranked based on $-log(pvalue)$ times the sign of the fold change. The tested pathways were part of the hallmark gene sets

of the Molecular Signatures Database (MSigDB). Transcription factor enrichment analysis was performed on the DEGs using the TRRUST Transcription Factors 2019 database.

***Assay for Transposase Accessible Chromatin (single cell ATAC seq):*** Liver from one *Spta*$^{sph/sph}$ and one *Spta*$^{wt/wt}$mouse were digested and macrophages isolated using F4/80 antibody-coated magnetic Dynabeads. Nuclei were isolated using the Nuclei Isolation for Single Cell ATAC sequencing (10x genomics) protocol, counted and loaded in the chromium controller. They were then processed according to the chromium next GEM single Cell ATAC reagent Kits v1.1 protocol. Libraries were pooled equimolarly and sequenced using a NextSeq 500 system according to 10x genomics recommendation. Sequencing depth of 25'000 read pairs per nucleus (paired-end, dual indexing). Read 1N: 50 cycles, i7 Index: 8 cycles, i5 Index: 16 cycles, Read 2N: 50 cycles.

Data was then processed using CellRanger ATAC suite (v1.2.0) from 10x genomics. Read filtering, alignement, barcode counting was done using cellranger-atac count and cellranger-atac aggr was used to merge the two samples. Data was further processed in R using the seurat package *Signac* (v0.2.4) (16, 17) and Seurat (3.1.5) (18, 19). Quality control was assured using a serie of per-cell metrics from the output of CellRanger: total number of fragments per peaks (>3000, <20'000), fraction of fragments in peaks (>15%), ratio reads in blacklist sites according to the ENCODE project (<5%) and nucleosome banding pattern (<10%) as well as transcription start site (TSS) enrichment scores according to ENCODE project (>2) computed using the *TSSEnrichement()* function of *Signac*. Normalization was done with a term frequency-inverse document frequency (TF-IDF) normalization using the *RunTFIDF()* function. Dimensional reduction was performed using singular value decomposition (SVD) on the TD-IDF normalized matrix with the r*unSVD()* function using all features (no previous feature selection step). UMAP non-linear dimension reduction was performed using *RunUMAP()* function and clustering with *FindNeighbors()* and *Finclusters()* functions with the SLM algorithm. A pseudo-gene expression matrix was created using the *FeatureMatrix()* function by counting the number of fragments for each cell that map to gene encoding regions of the mouse genome from EnsembleDB including the 2kb upstream region from them. This includes the gene coding region as well as the promoter region whose accessibility can be interpreted as correlated to gene expression. Cell types for each clusters were determined using this pseudo-gene expression matrix. Differentially accessible peaks between KCs and erythrophagocytes was performed using the *FindMarkers()* function

on the peak region fragment matrix. Peak coordinates were mapped to genes using the *Closestfeature()* function with EnsDb.Mmusculus.v79. Motif enrichment analysis was performed using the *Findmotifs()* function on the differentially accessible peaks with a list of motif position frequency matrices from the JASPAR 2018 database (20). *MotifPlot()* function was then used to generate the plots of the position weight matrices for the top overrepresented motifs. Raw and processed single-cell ATAC-sequencing data were submitted to the Gene Expression Omnibus (GEO) database repository (8, 9) .

***Gene array and RT-qPCR analysis***

***Microarray experiments and data analysis:*** Total RNA was isolated using the RNeasy Mini Kit according to the manufacturer's instructions, which included an on-column DNA digestion step (RNase-Free DNase Set; Qiagen, Hombrechtikon, Switzerland). To ensure that only high-quality RNA (RNA integrity number > 7.0) was used for gene expression analysis, each RNA sample was checked on an RNA Nanochip with a Bioanalyzer 2100 (Agilent Technologies). RNA was quantified spectrophotometrically with a NanoDrop ND-1000 spectrophotometer (NanoDrop Technologies, Wilmington, DE, USA). Fluorescently labeled cRNA was generated from 500 ng of total RNA with the Quick Amp Labeling Kit (Agilent Technologies) according to the manufacturer's protocol, and differential gene expression profiling was performed by competitive dual-color hybridization on whole-mouse or whole-human genome oligo microarrays (mouse: G4846A, 4 × 44 K, Agilent Technologies). Array slides were XDR-scanned and analyzed with Feature Extraction Software Version 10.7.3.1 (Agilent Technologies). Statistical analysis and visualization were performed with JMP Genomics 7.0 (SAS Institute, Boeblingen, Germany). Full gene array data were submitted to the Gene Expression Omnibus (GEO) database repository.

***Real-time PCR:*** Total RNA was isolated using the RNeasy Mini Kit according to the manufacturer's instructions (Qiagen, Hombrechtikon, Switzerland, 74106). Reverse transcription was performed with TaqMan reverse transcription reagents (Life Technologies, Basel, Switzerland, N8080234). Real-time PCR was performed using Fast SYBR™ Green Master Mix (Applied Biosystems, 4385612) to determine the expression levels of the target genes using the primers listed in the table below. Relative mRNA levels were calculated by the 7500 Fast System Sequence Detection Software Version 1.4 (Applied Biosystems) after normalization of each experimental sample to *Hprt* levels.

1. Mouse primers:

| TARGET GENES | FW primer | REV primer |
|---|---|---|
| *Hmox1* | aggctaagaccgccttcct | tgtgttcctctgtcagcatca |
| *Nqo1* | agcgttcggtattacgatcc | agtacaatcagggctcttctcg |
| *Slc7a11* | gattcatgtccacaagcacac | gagcatcaccatcgtcagag |
| *Il-6* | gctaccaaactggatataatcagga | ccaggtagctatggtactccagaa |
| *Tnf* | tcttctcattcctgcttgtgg | gaggccatttgggaacttct |
| *Il-12b* | aaggaacagtgggtgtccag | gttagcttctgaggacacatcttg |
| *Il-1b* | agttgacggaccccaaaag | agctggatgctctcatcagg |
| *Ifnb* | ctggcttccatcatgaacaa | agagggctgtggtggagaa |
| *Ifng* | atctggaggaactggcaaaa | ttcaagacttcaaagagtctgagg |
| *Cxcl9* | cttttcctcttgggcatcat | gcatcgtgcattccttatca |
| *Cxcl10* | gctgccgtcattttctgc | tctcactggcccgtcatc |
| *Ccl2* | catccacgtgttggctca | gatcatcttgctggtgaatgagt |
| *Ccl5* | tgcagaggactctgagacagc | gagtggtgtccgagccata |
| *Spic* | ccacttggttttcctgaacgtg | tgcggaaatgtcagcgagta |
| *Hprt* | cctcctcagaccgcttttt | aacctggttcatcatcgctaa |
| *Nos2* | gcatcccaagtacgagtggt | ccatgatggtcacattctgc |
| *Cd74* | caccgaggctccacctaaag | ttaccgttctcgtcgcactt |
| *Marco* | ttctgtcgcatgctcggtta | cagatgttcccagagccacc |
| *H2-Aa* | aagctttgacccccaaggtg | ggagcctcattggtagctgg |
| *H2-Ab1* | acggtgtgcagacacaacta | cgacattgggctgttcaagc |
| *H2-Eb1* | acggtgtgcagacacaacta | gtcaccgtaggctcaactct |
| *H2-T24* | ttacccgaactgaccctcca | attcaactgccaggtcaggg |
| *Gsr* | ctatgacaacatccctactgtggt | cccatacttatgaacagcttcgt |
| *Hba-a1* | tgtggatcccgtcaacttcaa | tgctcacagaggcaaggaat |

2. Human primers:

| TARGET GENES | FW primer | REV primer |
|---|---|---|
| *HPRT* | tgaccttgatttattttgcatacc | cgagcaagacgttcagtcct |
| *HO-1* | aggccaagactgcgttcct | ggtgtcatgggtcagcagc |
| *NQO1* | gggatccacggggacatgaatg | atttgaattcgggcgtctgctg |
| *IL-6* | tacagggagagggagcgata | ctcagacatctccagtcctct |
| *CXCL9* | tgagaaagggtcgctgttcc | gggcttggggcaaattgttt |
| *CXCL10* | aagtggcattcaaggagtacct | acacgtggacaaaattggct |
| *IL-12b* | cctgcccagagcaagatgtg | agttcccatatggccacgag |

**REFERENCES**

1. Scarborough J et al. Preclinical validation of the micropipette-guided drug administration (MDA) method in the maternal immune activation model of neurodevelopmental disorders [Internet]. *Brain Behav. Immun.* [published online ahead of print: April 9, 2020]; doi:10.1016/j.bbi.2020.04.015

2. Schaer DJ et al. CD163 is the macrophage scavenger receptor for native and chemically modified hemoglobins in the absence of haptoglobin. *Blood* 2006;107(1):373–380.

3. Schindelin J et al. Fiji: an open-source platform for biological-image analysis. *Nat. Methods* 2012;9(7):676–682.

4. Jui-Cheng Yen, Fu-Juay Chang, Shyang Chang. A new criterion for automatic multilevel thresholding. *IEEE Trans. Image Process.* 1995;4(3):370–378.

5. Sezgin M, Sankur B. Survey over image thresholding techniques and quantitative performance evaluation. *JEI* 2004;13(1):146–165.

6. McCarthy DJ, Campbell KR, Lun ATL, Wills QF. Scater: pre-processing, quality control, normalization and visualization of single-cell RNA-seq data in R. *Bioinformatics* 2017;33(8):1179–1186.

7. Lun ATL, McCarthy DJ, Marioni JC. A step-by-step workflow for low-level analysis of single-cell RNA-seq data with Bioconductor. *F1000Res.* 2016;5:2122.

8. Edgar R, Domrachev M, Lash AE. Gene Expression Omnibus: NCBI gene expression and hybridization array data repository. *Nucleic Acids Res.* 2002;30(1):207–210.

9. Barrett T et al. NCBI GEO: archive for functional genomics data sets--update. *Nucleic Acids Res.* 2013;41(Database issue):D991–5.

10. Dobin A et al. STAR: ultrafast universal RNA-seq aligner. *Bioinformatics* 2013;29(1):15–21.

11. Li H et al. The Sequence Alignment/Map format and SAMtools. *Bioinformatics* 2009;25(16):2078–2079.

12. Love MI, Huber W, Anders S. Moderated estimation of fold change and dispersion for RNA-seq data with DESeq2. *Genome Biol.* 2014;15(12):550.

13. Robinson MD, McCarthy DJ, Smyth GK. edgeR: a Bioconductor package for differential expression analysis of digital gene expression data. *Bioinformatics* 2010;26(1):139–140.

14. McCarthy DJ, Chen Y, Smyth GK. Differential expression analysis of multifactor RNA-Seq experiments with respect to biological variation. *Nucleic Acids Res.* 2012;40(10):4288–4297.

15. Subramanian A et al. Gene set enrichment analysis: a knowledge-based approach for interpreting genome-wide expression profiles. *Proc. Natl. Acad. Sci. U. S. A.* 2005;102(43):15545–15550.

16. Adorf CS, Dodd PM, Ramasubramani V, Glotzer SC. Simple Data and Workflow Management with the signac Framework [Internet]. *arXiv [cs.DB]* 2016;http://arxiv.org/abs/1611.03543. cited

17. Adorf CS et al. *glotzerlab/signac [Internet]*. 2019:

18. Butler A, Hoffman P, Smibert P, Papalexi E, Satija R. Integrating single-cell transcriptomic data across different conditions, technologies, and species. *Nat. Biotechnol.* 2018;36(5):411–420.

19. Stuart T et al. Comprehensive Integration of Single-Cell Data. *Cell* 2019;177(7):1888–1902.e21.

20. Khan A et al. JASPAR 2018: update of the open-access database of transcription factor binding profiles and its web framework. *Nucleic Acids Res.* 2018;46(D1):D260–D266.